RSC Advances

ROYAL SOCIETY OF CHEMISTRY

www.rsc.org/advances

Bi_2S_3/ Poly(vinylidene fluoride) Composite with High Dielectric Constant and Unusual Low Dielectric Loss Based on Preferentially Oriented Fillers

Jie Liu, Yu Luo, Yao Wang, Yuan Deng*, Xitong Xie

Beijing Key Laboratory for Advanced Functional Materials and Thin Film Technology, School of Materials Science & Engineering, Beihang University, Beijing 100191, China

Abstract: The main challenge of capacitor is how to reconcile the contradiction of lowering the dielectric loss while maintaining high dielectric constant of polymer based composites. In this work, a novel two-phase ferroelectric polymer composite, consisting of semiconductive bismuth sulfide (Bi_2S_3) nanorods and poly(vinylidene fluoride) (PVDF) matrix, was fabricated by a sequence of casting, hot-stretching and hot-pressing techniques. Orderly polymer composites based on PVDF assembled with parallel aligned Bi_2S_3 nanorods were realized in the composites after a hot-stretching-pressing process. It's interesting to note that those orderly polymer composites exhibit excellent dielectric properties. Results show that the composites with oriented structure have high dielectric constant and unusual low dielectric loss. The parallel aligned Bi_2S_3 nanorods along the tensile-strain direction could be charged with the improvement of dielectric properties of the composites. This study also provides an extremely useful method to reduce the dielectric loss of similar kind of composites.

* Corresponding author. Tel: +86-10-82313482; fax: +86-10-82313482.
E-mail address: dengyuan@buaa.edu.cn (Y. Deng).

Keywords: Dielectric properties; One-dimensional structure; Structure design; Bi_2S_3/PVDF composites;

1. Introduction

The polymer-matrix composites filled with inorganic particles such as ferroelectric ceramic [1, 2] and metal particles [3, 4] have attracted great attention due to their easy processing and flexibility for various potential applications such as embedded capacitors, actuators, and printed circuit boards [5-7]. Xu et al. prepared the semiconductor composites by mixing PVDF and various conductive fillers were investigated with regard to the dielectric constant as a function of frequency, temperature and the concentration of fillers[8]. Poly (vinylidene fluoride) (PVDF), which is flexible, easy to process and shows excellent electric breakdown properties, has become the subject of many intensive investigations for their broad applications in electromechanical systems [9, 10].

Many studies show that dielectric constant would be largely enhanced when mental and/or ceramic fillers were employed into the polymer based composites [11-15]. Dang et al. have prepared high-K CCTO/PI functional hybrid films, a high dielectric constant (49) is obtained at 10^2 Hz when the concentration of the CCTO filler reaches 40 vol%[16]. But the researchers note that, the reliability is of great importance for capacitor. Therefore, it is urgent to seek a kind of material, which can achieve high dielectric constant and low dielectric loss at low content. One important approach to improve the dielectric properties of composites is incorporating ceramic nanoparticles into polymer matrix to enhance their relatively permittivities. For instance, L. Zhang

et al. have prepared BST–P(VDF–CTFE) 0–3 nanocomposites, for the composites with 40 vol% of BST, a dielectric constant of 70 with a loss of 0.07 at 1 kHz is obtained at room temperature[17]. Sodano et al. reported a $BaTiO_3$ nanowires/PVDF composite with a dielectric constant of about 44.3, when the concentration of the conducting filler is 30 vol% [18]. However, the volume fraction of ceramic particles is usually very high, which will do great damage to the mechanical properties of polymer based composites [19].

To overcome the above shortcoming, inorganic conductors are often employed to increase the dielectric constant of polymer matrix based on the percolation theory[20]. However, the corresponding loss and leakage current of these composites are too high to meet the requirements of realistic applications. The one-dimensional fillers caused wide attention because of their large aspect ratio [21], so that the composites with these fillers can reach the percolation threshold at low content. Zhang et al. found that the fitting constant f_c increases with increasing frequency and they believed that this arises from the critical phenomenon, $\varepsilon_{eff} \propto f^{\gamma-1}$, for composites close to the f_c[22]. Nan et al. reported the dielectric properties of PVDF/ Bi_2S_3 nanorod (nr- Bi_2S_3) composites and the dielectric constant can reach 160 [23]. However, it is found that the dielectric loss of these percolative composites is usually quite high. Because the nanoscale fillers with large aspect ratio are partial to connect each other and form a conductive network with the increasing of conduct fillers, which would be blamed for the electric leakage loss. At the low frequency, the electric leakage could be considered to make the major contribution to the dielectric loss [24]. As a result, the dielectric loss of these

percolative composites is usually high when the percolation threshold was achieved[25]. And what really impacts the practical use of these percolative composites materials is dielectric loss, which is rarely mentioned and deserves more attention.

Therefore, the main challenge is how to reconcile the contradiction of lowering the dielectric loss while maintaining high dielectric constant. There are many methods to lower the dielectric loss of nanocomposites, such as, treating the nanoparticles with coupling agents [26, 27]; fabricating nanocomposites via in situ olefin polymerization and employing core@shell structured fillers. Xie et al. successfully lower the dielectric loss of polymer nanocomposites by using core–satellite structured ultra-small silver (Ag) decorated barium titanate (BT) nanassemblies [28]. Nowadays, structure design, as a new method to improve the dielectric properties of polymer composites has been draw wide attention. Our previous results showed that the addition of Bi_2S_3 could enhance the dielectric properties of the PVDF and polyethylene (PE) [29, 30]. We also have fabricated an orderly polymer composite with zinc flakes (ZFs) oriented parallel in the PVDF, which obtained high dielectric constant of 176 but low loss of 0.06 at 10^3 Hz [31]. Along this line, we expect to prepare one-dimensional directional composites by structure design, which has high dielectric constant and low dielectric loss at low content.

Tensile strain is usually employed to enhance the tensile strength and modulus of polymer composites [32]. Very few studies have been focused on the effect of tensile strain on dielectric properties. Yao et al. studied the tensile strain's effect on the dielectric properties of multiwall carbon nanotube (MWNT)/poly(vinylidenefluoride)

(PVDF) nanocomposites, the maximum increment in the dielectric constant of the composite can reach 30% at 10^2 Hz relative to that before stretching[33]. Dang et al. have studied the effect of tensile strain on morphology and dielectric property in nanotube/polymer nanocomposites [34], the dielectric constant and conductivity always decreased after the composites were stretched. So in this work, the novel but simple method (hot-stretching and hot-pressing) is developed to lower the dielectric loss of the two-phase Bi_2S_3/PVDF composites while maintaining the high dielectric constant. By designing such a one-dimension well-aligned parallel structure, a significant reduction in dielectric loss of the novel two-phase Bi_2S_3/PVDF composite is observed, while the dielectric constant remains a high level at a lower content.

2. Materials and methods

Bi_2S_3 nanorods were synthesized by a hydrothermal method [35]. All Bi_2S_3 nanorods in this work were treated by surfactant γ-aminopropyltriethoxysilane (KH550). The composites were prepared by a simple solution-casting, hot-stretching and hot-pressing method. First, a desired amount of Bi_2S_3 nanorods was ultrasonicated in 20 ml N, N-dimethylformamide (DMF) solvent for 30min, and at the same time, a certain amount of PVDF was dissolved in N, N-dimethylformamide (DMF) at room temperature. Next, PVDF solution was added into Bi_2S_3 suspension solution when the latter was stirred. The mixture was further stirred for 2h, and ultrasound was applied to the suspension more than one time in order to prevent the agglomeration of Bi_2S_3 nanorods. Then the composite films were made by the solution casting machine at 80 ℃, using glass as substrate. The resultant films were

stretched about 4 times along the casting direction at 160 ℃. Finally, the Bi_2S_3/PVDF films were cut into 10×10 mm pieces, these little pieces of the oriented samples (O-S) were stacked up along the tensile strain direction (the disoriented samples (D-S) with no direction) into the hot-press mould, the bulk samples were made by a simple hot-pressing method at 200 ℃, under 4 MPa (heated for 10 min at the same temperature, pre-pressed for 15 min, released for a while, and then re-pressed for 15 min, followed by cooling to room temperature under the same pressure). For electrical measurement, silver electrodes were painted on both sides of the samples.

The fractured surface morphology of the samples was examined by scanning electron microscopy (FEI Siron 200). The dielectric properties were measured by employing an Agilent 4294A Impedance analyzer in the frequency ranges of 100 Hz–10 MHz at room temperature. The out-of-plane dielectric properties of the nanocomposites were studied in this work.

3. Results and discussion

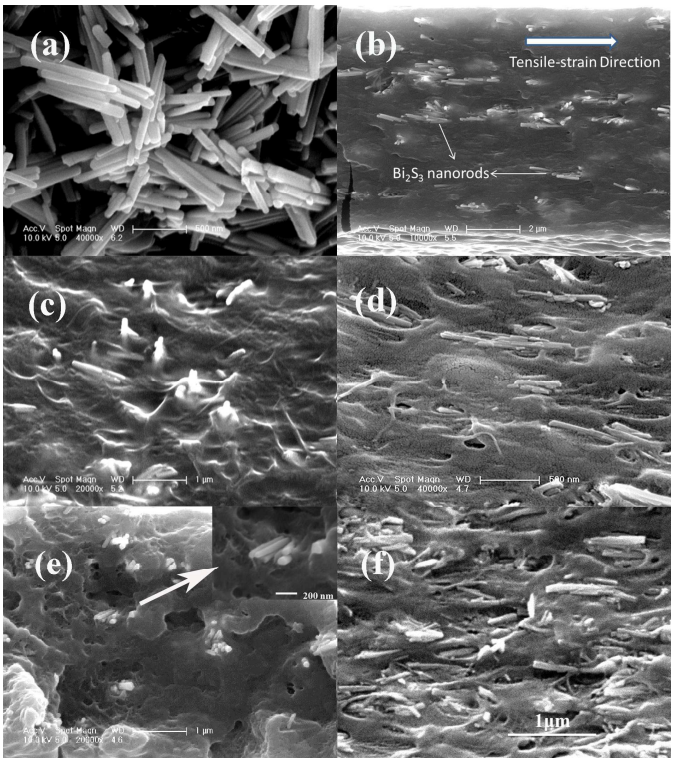

Fig. 1. SEM images of (a) Bi_2S_3 nanorods; and cross-section views of oriented or disoriented Bi_2S_3/PVDF composites with different f_{Bi2S3}: (b) 2 % O-S; (c) 2 % D-S; (d) 4 % O-S; (e) 2 % O-S (another direction); (f) 10 % O-S.

Bi_2S_3 nanorods were synthesized by a hydrothermal method. The SEM micrograph of Bi_2S_3 nanorods and Bi_2S_3/PVDF composites are shown in Fig. 1. From Fig. 1a, the hydrothermal synthesized products mainly consist of various sizes of Bi_2S_3 nanorods with lengths of 0.4–1 μm and diameters of 80–100 nm, and the aspect ratio is about 10.

The composite films were fabricated by casting procedure at 80 ℃. The cross-section micrograph Fig. 1(b-c) of the composite samples demonstrate that the Bi_2S_3 nanorods are homogeneously dispersed into the PVDF matrix without serious aggregation at low Bi_2S_3 nanorods content, i.e., f_{Bi2S3}=2 vol%. However, as f_{Bi2S3} increases, some Bi_2S_3 aggregates emerge, as shown in Fig. 1d (f_{Bi2S3}=4 vol%) and Fig. 1f (f_{Bi2S3}=10 vol%). The films were stretched along the casting direction at 160 ℃.

After been stretched, the nanorods have preferential orientations in the direction parallel to the tensile strain, which could be clearly seen in the cross-section micrograph Fig. 1(b, d, and f).

As shown in Fig. 1e, numerous cross surface of Bi_2S_3 nanorods could be noticed, and whole nanorods can barely be seen in the picture because this cross-section is perpendicular to the tensile-strain direction. The holes in this picture should be attributed to the extraction of the Bi_2S_3 nanorods, because the size of the hole is basically consistent with the diameter of the Bi_2S_3 nanorods and there are no clear holes in Fig. 1b. By contrast, no preferential orientations of Bi_2S_3 nanorods could be observed in the disoriented samples (D-S) (see Fig. 1c). Due to the big difference of the tensile strength and modulus of the PVDF matrix and Bi_2S_3 nanorods fillers, the stretching process will do great damage to the interface between the matrix and the fillers of the nanocomposite and decreased the dielectric properties. But there are no clearly defects can be seen in Fig.1b at low Bi_2S_3 nanorods content, which explain that the hot-stretching process can fix the defects at high temperature above PVDF viscoelastic temperature. In the hot-stretching process, we call this phenomenon as the effect of "self-repairing" when the matrix material (PVDF) is at its viscoelastic temperature.

From Fig. 1 we can draw a conclusion that the tensile strain played a crucial role in deciding the morphology of Bi_2S_3/PVDF nanocomposites. After that, a pressure at 200℃ was added along the direction perpendicular to the film plane when the film was cut into pieces, and then were stacked up along the tensile strain direction (the

disoriented samples with no direction) into the hot-press mould. The hot-pressing progress could effectively reduce the bubble defect in the composite.

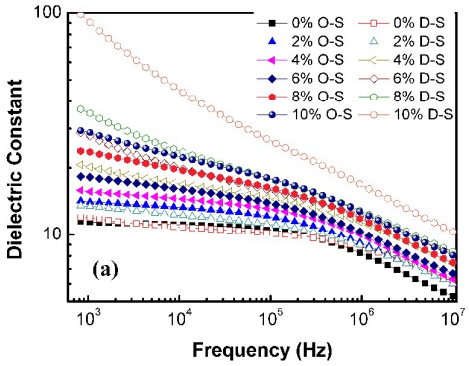

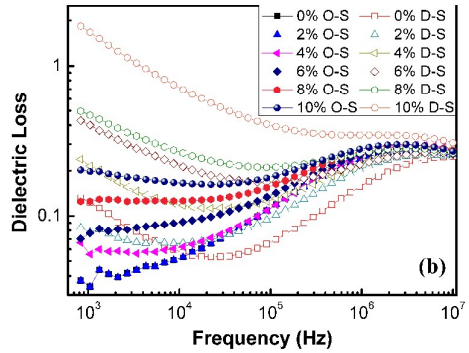

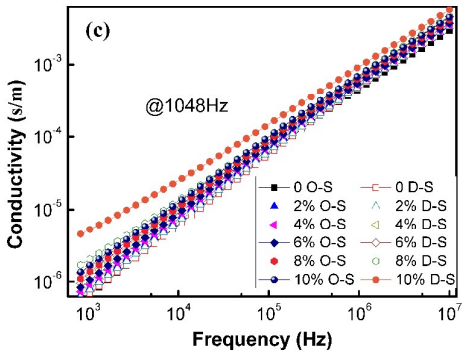

Fig. 2. Frequency-dependence of: (a) dielectric constant, (b) dielectric loss and (c) conductivity of the oriented and disoriented Bi_2S_3/PVDF composites with different f_{Bi2S3} at room temperature.

Fig. 2 shows the dependences of dielectric constant, dielectric loss and

conductivity of the Bi_2S_3/PVDF composites with different concentrations of Bi_2S_3 nanorods with oriented structure and disoriented structure on frequency at room temperature. A conclusion can be drawn that the dielectric constant, dielectric loss and conductivity of the composites always increased with the increasing Bi_2S_3 nanorods, whether the Bi_2S_3 nanorods are oriented or not. The dielectric constant of the composites always decreased with the increasing frequency, while the conductivity is increased. At low frequency range, according to the interfacial polarization or Maxwell– Wagner–Sillars effect [36], because of the different relaxation time of the PVDF and Bi_2S_3 nanorods, lots of free charge carriers generated by surface polarization are blocked at the interfaces between Bi_2S_3 nanorods and PVDF matrix, and lots of dipoles form on the Bi_2S_3 nanorods. The inertia of formed dipoles makes the polarization spend much more time than other dielectric process, thus, the interfacial polarization occurs at low frequency, and dielectric constant and loss decrease rapidly when frequency increases. At high frequency range, the electrical properties of the composites are dominated by the PVDF. Therefore, the dielectric constant is comparatively independent of frequency and is generally lower than that at low frequency, and the dielectric properties of the Bi_2S_3/PVDF nanocomposites change little by the tensile strain at high frequency.

Fig. 3 shows the schematic images of how tensile-strain effects the Bi_2S_3 nanorods distribution in polymer composites. The (a) and (a') is disoriented and oriented simples at low content filling, while (b) and (b') is disoriented and oriented simples at high content filling, respectively. Because the Bi_2S_3 nanorod was an

anisotropic rod material with a large aspect ratio, the nanorods would be rearranged along the tensile-strain direction when the Bi_2S_3/PVDF composites are stretched. This mechanism has been verified by the SEM micrographs as is shown in Fig. 1.

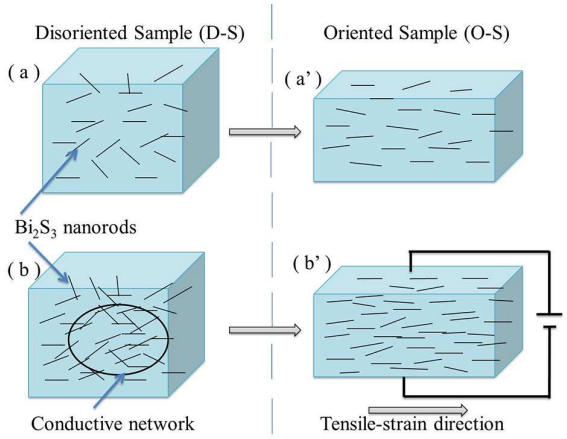

Fig. 3. Schematic images of Bi_2S_3 nanorods distribution in polymer composites at low content filling (a) and (a') and high content filling (b) and (b') of Bi_2S_3 nanorods with disoriented structure (a) and (b) and oriented structure (a') and (b'), respectively.

It is well known that the enhancement of dielectric constant in the low frequency range is mainly due to the contribution of interfacial polarization associated with the entrapment of space charges at the interfaces of fillers and matrix. Therefore, the anisotropic dielectric constant could be ascribed to the anisotropic intensity of interfacial polarization. According to the theory of dielectrics, the polarization intensity P is defined as [31]

$$P = \frac{\sum \mu}{V} = \frac{\sum ql}{V} \qquad (1)$$

where μ stands for the dipolar moment, V corresponds to the volume of the sample, q and l are denoted as positive or negative charge and the displacement between positive and negative charges under external electric field, respectively. In the case of interfacial polarization, positive or negative space charge q and volume V of a given

cubic sample are considered as constants independent of directions.

As is shown in Fig. 3, after been stretched, the distance between the Bi_2S_3 nanorods is greatly reduced in the direction of perpendicular to the tensile strain. Therefore, the displacement *l* of the oriented samples is obviously higher than that of the disoriented samples in the perpendicular direction, which leading to the stronger intensity of interfacial polarization and higher dielectric constant. Simultaneously, with the increase of Bi_2S_3 nanorods, a fast increase of dielectric constant can be found in the disoriented samples (see Fig. 4a).

According to the percolation theory, when f_{Bi2S3} is less than f_c, the dielectric constant (ε) near the percolation threshold can be characterized by the power law[20, 37], as follows:

$$\varepsilon(f_{Bi2S3}) \propto (f_c - f_{Bi2S3})^{-s} \quad \text{as} \quad f_{Bi2S3} < f_c \qquad (2)$$

where s is the dielectric critical exponent. For disoriented samples, the inset in Fig. 4(a) shows that the linear fit of the experimental data according to Eq. (2) and f_c =10.9% and s=0.80, and s agrees well with the universal value (0.7-1). As for oriented samples, the percolation threshold is very large, which can be clearly seen in Fig. 4(a).

See from Fig. 4, at 1048 Hz, with the increasing of the concentration of Bi_2S_3 nanorods, the differences of dielectric constant and dielectric loss between the oriented and disoriented composites become more significant. At 1048 Hz, for f_{Bi2S3}=4 vol%, the dielectric loss of the disoriented sample is 0.21472 which is about 3 times higher than that of oriented sample (0.05561). However, when f_{Bi2S3} increases to 10 vol%, the dielectric loss of the disoriented sample is 1.672 which is almost 9 times of

that of the oriented sample (0.1975).

The conductive network is very important to improve the dielectric constant as well as dielectric loss of composites. When f_{Bi2S3} is low, most of the Bi_2S_3 nanorods are fully dispersed in the matrix without serious aggregation, which may be due to the solvent evaporation process. Tensile strain cannot do much under this circumstance, so the change of the dielectric properties of these two series composites are not obvious (see Fig. 4). But the Bi_2S_3 nanorods begin to connect to each other and form a conductive network with the increasing of the volume content. In this case, the conductive network would be destroyed by the tensile strain, because the Bi_2S_3 nanorods prefer to stay along the tensile strain direction and parallel to each other when the tensile strain is employed, which decrease the chance to connect each other.

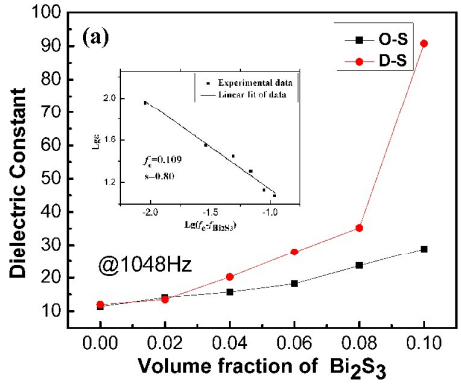

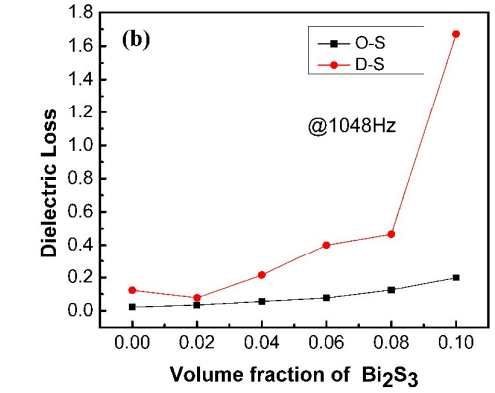

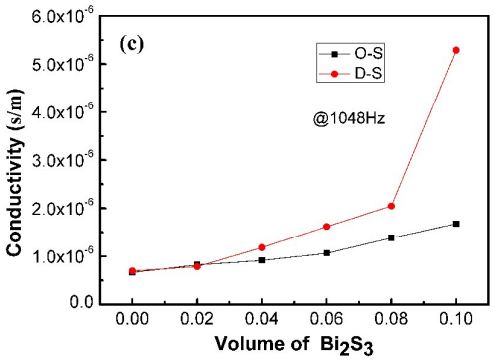

Fig. 4. At 1048 Hz, the dependence of (a) dielectric constant, and the inset in (a) presents the best fitting of dielectric constants of disoriented samples according to Eq. (1); (b) dielectric loss and (c) conductivity of the oriented and disoriented Bi_2S_3/PVDF composites on the f_{Bi2S3}, measured at room temperature.

There is a gradual enhancement of dielectric constant with increasing f_{Bi2S3} with low loading of Bi_2S_3 nanorods. However, when $f_{Bi2S3} > 0.08$, both the dielectric constant and dielectric loss of the disoriented composites have a dramatic enhancement, while the oriented composites don't have. With the increasing Bi_2S_3 nanorods, the conductive phase Bi_2S_3 nanorods began to connect, and form the conductive network where the dielectric constant abruptly increases. When the conductive network formed, the leakage current increased dramatically, so the dielectric loss also abruptly increased. Because of the tensile strain, the oriented composites did not appear this phenomenon. The oriented composites need much

more Bi_2S_3 nanorods to form the conductive network, which means the hot-stretching process delayed the percolation threshold of the composites. This could be explained by the rearrangement of Bi_2S_3 nanorods in the composites which destroyed the network structures. In this case, numerous clusters were broken off, and subsequently the Bi_2S_3 nanorods were rearranged along the tensile-strain direction as a preferential orientation. Namely, numerous Bi_2S_3 nanorods in the composites were parallel to the tensile-strain direction after stretched. As a result, the dielectric constant and conductivity of Bi_2S_3/PVDF nanocomposites decreased significantly.

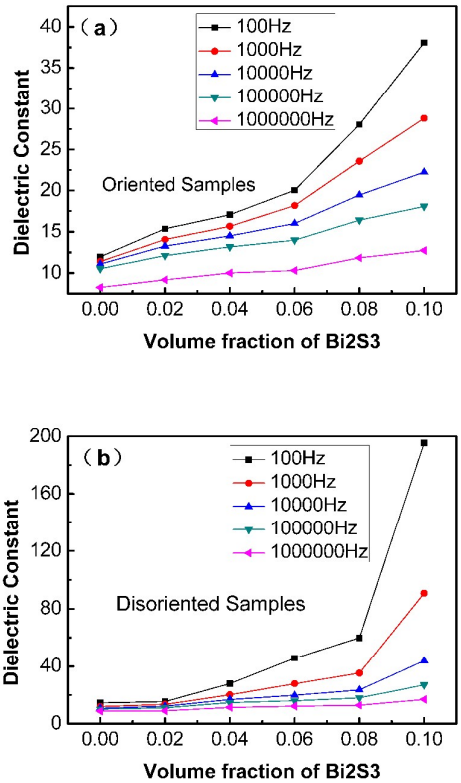

Fig. 5 The change in dielectric constant with the filled content of Bi2S3 nanorods at different frequencies.

The change in dielectric constant with the filled content of Bi_2S_3 nanorods at different frequencies is shown in Fig. 5. The dielectric constant increases with the

increasing f_{Bi2S3} at all considered frequencies, which is due to the conductivity increase of semiconductive Bi_2S_3 nanorods. As the frequency increases, the dielectric constant increases slowly for these two kinds of composites. At low frequency, the molecules have enough time for polarization. However, at high frequency, the polarization of molecules does not have enough time to catch up with the change in electrical field frequency, which leads to the weak dependence of dielectric constant on the filled content[29]. Compare Fig. 5a with Fig. 5b, we can draw that the dielectric constant of the D-S deceased more intense than that of the O-S, as we have mentioned before.

4. Conclusions

In summary, orderly polymer composites based on PVDF assembled with parallel aligned Bi_2S_3 nanorods were prepared by simple and robust techniques of hot stretch-pressing process. It's interesting to note that those orderly polymer composites indicate excellent dielectric properties with high dielectric constant and unusual low dielectric loss. The dielectric loss of the two-phase Bi_2S_3/PVDF composite decreased after the composites were stretched, while the dielectric constant still remains at high level. The dielectric loss of the 4 vol% oriented sample (O-S, f_{Bi2S3}=4 vol%) is lowered from 0.21472 to 0.05561 at 1048Hz due to the orientation of the Bi_2S_3 nanorods. While the dielectric constant of the 4 vol% oriented sample is still keep high to 15.6. The abruptly decrease in the dielectric loss of the percolative composite in the low frequency range could be attributed to the rearrangement of Bi_2S_3 nanorods along the tensile-strain direction in the Bi_2S_3/PVDF nanocomposites. In the

hot-stretching process, the nanocomposite materials have the effect of "self-repairing" when the matrix material (PVDF) is at its viscoelastic temperature. This study provides a useful but simple method to reducing the dielectric loss of the composites materials which are constituted by thermoplastic polymer matrix and fillers with large aspect ratio.

Acknowledgements

The work was supported by National Natural Science Fund Innovation Group (No.**51221163**), Research Fund for Doctor Station Sponsored by the Ministry of Education of China (20111102110035) and the Fundamental Research Funds for the Central Universities.

References:

1. D. Yu, N. Xu, L. Hu, Q. Zhang and H. Yang, *J MATER CHEM C*, 2015, **3**, 4016-4022.
2. H. Hao, M. Liu, H. Liu, S. Zhang, X. Shu, T. Wang and Z. Y. A. M. Cao, *RSC ADV*, 2015, **5,** 8868–8876.
3. W. Zhou, J. Zuo and W. Ren, *Composites: Part A*, 2012, **43**, 658-664.
4. D. Bhadra, S. C. Sarkar and B. K. Chaudhuri, *RSC ADV*, 2015, **5**, 36924–36932.
5. W. Jillek and W. K. C. Yung, *INT J ADV MANUF TECH*, 2005, **25**, 350-360.
6. Z. Dang, J. Yuan, S. Yao and R. Liao, *ADV MATER*, 2013, **25**, 6334-6365.
7. M. Panda, V. Srinivas and A. K. Thakur, *APPL PHYS LETT*, 2011, **99**, 42905.
8. H. Xu, H. Xie, D. Yang, Y. Wu and J. Wang, *Journal of Applied Polymer Science*, 2011, **122**, 3466–3473.
9. Y. Zhen, J. Arredondo and G. Zhao, *Open Journal of Organic Polymer Materials*, 2013, **03**, 99-103.
10. Z. Dang, J. Yuan, S. Yao and R. Liao, *ADV MATER*, 2013, **25**, 6334–6365.
11. H. A. Ávila, L. A. Ramajo, M. S. Góes, M. M. Reboredo, M. S. Castro and R. Parra, *ACS APPL MATER INTER*, 2013, **5**, 505-510.
12. Z. Dang, J. Yuan, J. Zha, T. Zhou, S. Li and G. Hu, *PROG MATER SCI*, 2012, **57**, 660-723.
13. C. W. Beier, J. M. Sanders and R. L. Brutchey, *The Journal of Physical Chemistry C*, 2013, **117**, 6958-6965.
14. J. Li, S. I. Seok, B. Chu, F. Dogan, Q. Zhang and Q. Wang, *ADV MATER*, 2009, **21**, 217-221.
15. X. Xiao, H. Yang, N. Xu, L. Hu and Q. Zhang, *RSC ADV*, 2015, **5**, 79342–79347.
16. Z. Dang, T. Zhou, S. Yao, J. Yuan, J. Zha, H. Song, J. Li, Q. Chen, W. Yang and J. Bai, *ADV MATER*, 2009, **21**, 2077–2082.
17. L. Zhang, P. Wu, Y. Li, Z. Y. Cheng and J. C. Brewer, *Composites Part B: Engineering*, 2014, **56**, 284-289.
18. H. Tang, Z. Zhou and H. A. Sodano, *ACS APPL MATER INTER*, 2014, **6**, 5450-5455.
19. D. Wang, T. Zhou, J. Zha, J. Zhao, C. Shi, Z. Dang, *J MATER CHEM A*, 2013, **1**, 6162-6168.

20. C. W. Nan, Y. Shen and J. Ma, *Annual Review of Materials Reserach*, 2010, **40**, 131-135.
21. R. L. Poveda and N. Gupta, *MATER DESIGN*, 2014, **56**, 416-422.
22. L. Zhang, P. Bass and Z. Y. Cheng, *APPL PHYS LETT*, 2014, **105**, 42905.
23. N. Ning, X. Bai, D. Yang, L. Zhang, Y. Lu, T. Nishic and M. Tian, *RSC ADV*, 2014, **4**, 4543–4551.
24. B. P. Sahoo, K Naskar, R Choudhary, S Sabharwal, D Tripathy.*J APPL POLYM SCI*, 2012, **124**, 678–688.
25. M. Panda, V. Srinivas and A. K. Thakur, *APPL PHYS LETT*, 2008, **92**, 132905.
26. P. Kim, N. M. Doss, J. P. Tillotson, P. J. Hotchkiss, M. Pan, S. R. Marder, J. Li, J. P. Calame and J. W. Perry, *ACS NANO*, 2009, **3**, 2581-2592.
27. P. Kim, S. C. Jones, P. J. Hotchkiss, J. N. Haddock, B. Kippelen, S. R. Marder and J. W. Perry, *ADV MATER*, 2007, **19**, 1001-1005.
28. L. Xie, X. Huang, B. Li, C. Zhi, T. Tanaka and P. Jiang, *PHYS CHEM CHEM PHYS*, 2013, **15**, 17560.
29. Y. Deng, Y. Zhang, Y. Xiang, G. Wang and H. Xu, *Journal of Materials Chemistry*, 2009, **19**, 2058.
30. Y. Deng, N. Li, Y. Wang, Z. Zhang, Y. Dang and J. Liang, *MATER LETT*, 2010, **64**, 528-530.
31. Y. Zhang, Y. Wang, Y. Deng, Y. Guo, W. Bi, M. Li, Y. Luo and J. Bai, *APPL PHYS LETT*, 2012, **101**, 192904.
32. Y. Gao, Q. Fu, L. Niu, Z. Shi. *J MATER SCI*, 2015, **50**, 3622-3630.
33. S. Yao, J. Yuan, T. Zhou, Z. Dang and J. Bai, *The Journal of Physical Chemistry C*, 2011, **115**, 20011-20017.
34. Z. Dang, S. Yao, H. Xu. *APPL PHYS LETT*, 2007, **90**, 12907.
35. J. Lu, Q. Han, X. Yang, L. Lu and X. Wang, *MATER LETT*, 2007, **61**, 3425-3428.
36. Z. Dang, L. Wang, Y. Yin, Q. Zhang, Q. Lei. *ADV MATER*, 2007, **19**, 852-857.
37. Z. Dang, L. Z. Fan, Y. Shen and C. W. Nan, *CHEM PHYS LETT*, 2003, **369**, 95-100.